JOC The Journal of Organic Chemistry

Article

pubs.acs.org/joc

Cucurbit[10]uril-Based [2]Rotaxane: Preparation and Supramolecular Assembly-Induced Fluorescence Enhancement

Yang Yu,[†,§] Yawen Li,[†,§] Xiaoqing Wang,[†] Hao Nian,[†] Le Wang,[†] Jie Li,[†] Yanxia Zhao,[†] Xiran Yang,[‡] Simin Liu,*[,‡] and Liping Cao*[,†]

[†]Key Laboratory of Synthetic and Natural Functional Molecule Chemistry of the Ministry of Education, College of Chemistry and Materials Science, Northwest University, Xi'an, 710069, P. R. China

[‡]School of Chemistry and Chemical Engineering, Wuhan University of Science and Technology, Wuhan 430081, P. R. China

Supporting Information

ABSTRACT: As the cucurbit[*n*]uril (CB[*n*]) homologue with the largest cavity size, cucurbit[10]uril (CB[10]) can encapsulate big guests to form interesting host−guest complexes/assemblies. Herein, we report the preparation and fluorescence properties of CB[10]-based [2]rotaxane (CB[10]·**1**) formed from cucurbit[10]uril and dumbbell-like guest **1**. This [2]rotaxane (CB[10]·**1**) is assembled by C═O···N^+ ion−dipole interactions between oxygen atoms of the carbonyl fringed portals of CB[10] and the positively charged pyridinium units of **1** via the slipping method under heating at 95 °C in DMSO. In contrast, other cucurbit[*n*]uril (CB[*n*], *n* = 6−8) homologues cannot form rotaxanes with **1** due to their smaller cavities. The dumbbell-like guest **1** is a poor emitter in DMSO. Interestingly, the formation of CB[10]·**1** renders the restriction of intramolecular rotation of TPE, which features a strong fluorescent intensity, long lifetime, and high quantum yield. Furthermore, CB[10]·**1** is shown to aggregate plate-like structures with various sizes in different solvents (DMSO, THF, or $CHCl_3$), resulting in a stepwise aggregation-induced emission enhancement effect. This kind of CB[10]-based [2]rotaxane may be used to fabricate luminescent systems with unique emission properties.

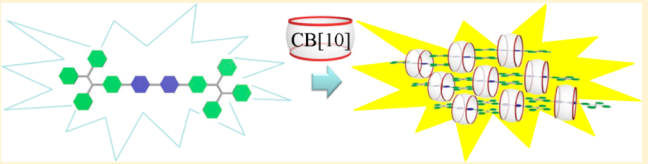

INTRODUCTION

Luminescent molecules or systems have attracted increasing interest due to their applications as optical devices,[1] photo-induced materials,[2] biological applications (imaging,[3] sensor,[4] and probes[5]), photodynamic therapy,[6] and molecular machines,[7] among other applications. The self-assembly of luminescent molecules[8] through noncovalent forces cause the change of luminescent properties, including excimer formation,[9] fluorescence resonance energy transfer (FRET),[10] aggregation-caused quench (ACQ),[11] aggregation-induced emission (AIE)/aggregation-induced emission enhancement (AIEE),[12] and J-/H-aggregation.[13] Inspired by these phenomena, supramolecular scientists, especially those who are interested in host−guest chemistry and material chemistry, have developed a series of new design strategies for tuning emission properties via host−guest recognitions to achieve functional systems, such as near-infrared materials[14] and energy transfer systems.[15]

Cucurbit[*n*]urils (CB[*n*]s),[16] a family of pumpkin-shaped macrocyclic molecules bearing a rigid hydrophobic cavity and two identical carbonyl fringed portals, are of great interest because of their excellent recognition property in water and wide applications in molecular recognition,[17] self-assembly,[18] catalysis,[19] biosensor,[20] drug delivery,[21] supramolecular polymer,[22] molecular machine,[23] and other supramolecular systems.[24] In particular, CB[*n*]s are also well-known to form complexes with a range of organic fluorophores, which cause profound changes in increasing fluorescent intensity, lifetime and quantum yield,[25] enhancing photothermal conversion,[6] and tuning fluorescent color[26] through host−guest interaction with their hydrophobic cavities in water. For examples, Kaifer and co-workers discovered that CB[7] could form stable host−guest complexes with cyanine dyes to achieve the emission off-on switch between the H- and J-aggregation.[27] Galoppini and co-workers described an unprecedented fluorescence enhancement of viologen derivative bound with two CB[7].[25c] Ni and co-workers reported a CB[8] across-linked supramolecular luminescent system with tunable and dynamical photophysical properties.[26]

As the CB[*n*] homologue with the largest cavity size, cucurbit[10]uril (CB[10]) is unique because of its ability to bind large guests within its cavity (Figure 1a).[28] For examples, Day, Isaacs, Collins, Wallace, and Liu found that CB[10] could encapsulate cucurbit[5]uril,[28a] calix[4]arene,[28b] triazene-arylene oligomer,[28c] metalloporhyrin,[28d] platinum/ruthenium/iridium polypyridyl complexes,[28e−g] and blue box,[28h] respectively. However, few reports were involved with the construction of a supramolecular luminescent system from CB[10] as a host in the solution.[28g] In this paper, we report the preparation and supramolecular assembly induced fluorescence enhancement of rotaxane CB[10]·**1** formed from CB[10] and a dumbbell-like

Received: February 20, 2017
Published: May 10, 2017

DOI: 10.1021/acs.joc.7b00400
J. Org. Chem. 2017, 82, 5590−5596

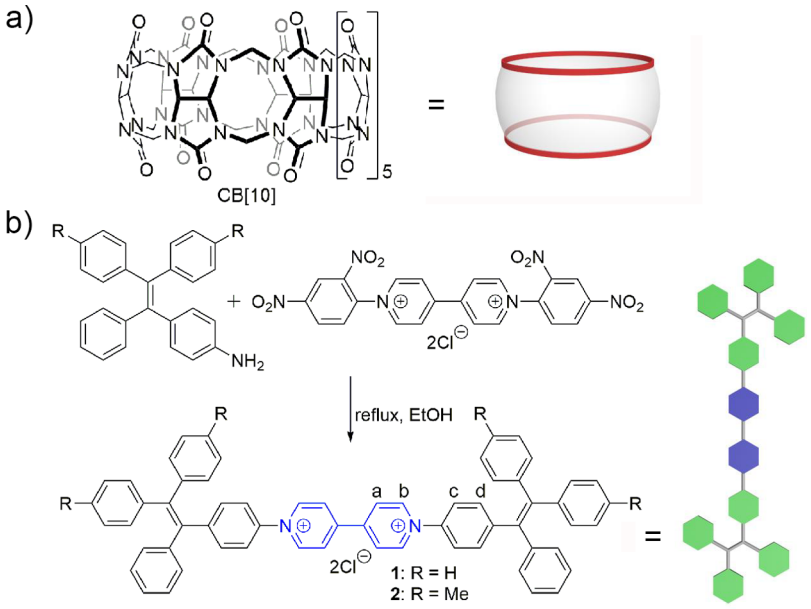

Figure 1. (a) Chemical structure of CB[10]; (b) synthesis of dumbbell-like guests **1**−**2**.

guest, 1,1′-ditetraphenylethenyl-4,4′-bipyridine-1,1′-diium dichloride (**1**), in DMSO. In this case, CB[10] imposes a structural confinement of guest **1**, resulting in the restriction of intramolecular rotation (RIR) of tetraphenylethylene (TPE) in CB[10]·**1** and increasing their electron density by ion−dipole interactions. These effects together improve fluorescent emission properties of this rotaxane system. At the same time, CB[10]·**1** further exhibits a stepwise aggregation-induced emission enhancement (AIEE) effect in different solvents (THF or $CHCl_3$).

RESULTS AND DISCUSSION

Design and Synthesis of Dumbbell-like Guests. As a mechanically interlocked molecule, a rotaxane must have a dumbbell-like molecule as an axle which is threaded through a macrocyclic molecule.[29] Recently, cucurbit[*n*]uril-based rotaxanes as supramolecular building blocks have been synthesized and used for the construction of sophisticated supramolecular architectures, such as infinite 1D lines,[30] 2D networks,[31] 3D frameworks,[32] and discrete molecular necklaces.[33] To prepare CB[10]-based rotaxane, a dumbbell-like molecule with a suitable recognition site for anchoring CB[10] and two large enough stoppers is required.

Viologen derivatives as the bis-cationic and aromatic guests are suitable recognition units for fabricating a mechanically interlocked complex with cucurbit[*n*]uril, which has a hydrophobic cavity for aromatic residues and two cyclic carbonyl portals for positively charged pyridinium units.[34] The tetraphenylethylene (TPE) moiety was incorporated for its AIE effect and also acts as a stopper. Therefore, we designed and synthesized two dumbbell-like guests, 1,1′-ditetraphenylethenyl-4,4′-bipyridine-1,1′-diium dichloride derivatives (**1**−**2**), containing a viologen unit in the middle for binding CB[10] and two TPE units at both terminals as the stopper and fluorophore. As shown in Figure 1b, guests **1**−**2** were synthesized by the reaction of corresponding monoamino TPE with *N*,*N*′-bis(2,4-dinitrophenyl) 4,4′-bipyridine-1,1′-diium chloride salt by the Zincke reaction, in 96% yield (see Supporting Information). We envision that guests **1**−**2** would undergo host−guest interaction with CB[*n*] to generate CB[*n*]-based rotaxane, resulting in the change of aggregation and the restriction of intramolecular rotation (RIR) of TPE to realize fluorescence enhancement.

Preparation of Rotaxane CB[10]·1. CB[*n*] compounds are slightly soluble in water and almost insoluble in common organic solvents, but solvent-soluble guests that are encapsulated in the cavities of CB[*n*]s usually can promote the solubility of CB[*n*]-based complexes. We found that the dumbbell-like guest **1** (chloride salt) was insoluble in water, but soluble in DMSO or MeOH. Therefore, we decided to investigate the host−guest recognition of **1** with CB[*n*] (*n* = 6−8, 10) by ^{1}H NMR in DMSO-d_6, even though CB[*n*]s had extremely poor solubility in DMSO-d_6. It is known that the diameter at the portal of CB[*n*] (*n* = 6−8) is 3.9, 5.4, and 6.9 Å, respectively.[16] Because the size of the TPE unit is about 7.4−9.0 Å, which is bigger than the size of CB[*n*] (*n* = 6−8),[35] they cannot encapsulate **1** even under heating at high temperature for several weeks. As a result, we failed to gain the rotaxanes from **1** and CB[*n*] (*n* = 6−8) via the slipping method (Figure S5).

Unlike smaller CB[*n*] (*n* = 6−8), CB[10] with the portal diameter of 9.5−10.6 Å and volume of ∼870 Å^3 could be threaded with the TPE unit to form a rotaxane via the slipping method. We observed a slowly slipping formation process of rotaxane CB[10]·**1** by ^{1}H NMR in DMSO-d_6. Figure 2 shows the ^{1}H NMR spectra recorded for guest **1** alone, as an initial mixture of **1** with CB[10], and as rotaxane CB[10]·**1**. Initially, the resonance peaks of free **1** did not change at all when 1 equiv of CB[10] was added into the solution of **1** in DMSO-d_6 at room temperature. Surprisingly, however, some tiny peaks belonging to bound **1** were observed when the mixture was heated at 95 °C for 2 days. At the same time, the resonance peaks of free and bound CB[10] became much clearer, indicating that the host−guest complex was coming up (Figure 2b). This phenomenon suggested that the unsubstituted TPE units of guest **1** were able to reversibly thread through CB[10] at higher temperature, and then the dynamic complex became kinetically trapped as a rotaxane at the lower temperature. The

DOI: 10.1021/acs.joc.7b00400
J. Org. Chem. 2017, 82, 5590−5596

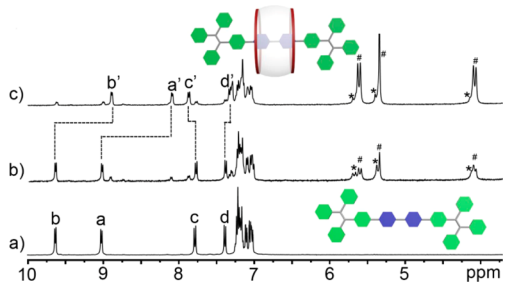

Figure 2. ^{1}H NMR spectra (400 MHz, DMSO-d_6, rt) for (a) **1**; (b) **1** (0.5 mM) and CB[10] (0.5 mM) at 95 °C for 2 days; and (c) **1** (0.5 mM) and CB[10] (0.5 mM) for 17 days at 95 °C. *Free CB[10] and #bound CB[10]. Here primes (′) denote protons binding with host.

positive result encouraged us to continue this experiment. Under heating at 95 °C for 17 days, it was shown that the resonance peaks of both free **1** and free CB[10] nearly disappeared and the resonance peaks of host–guest complex grew, which was strong evidence for the formation of rotaxane CB[10]·**1** in 81% yield (Figures 2c and S6). It also illustrated that the formation of rotaxane CB[10]·**1** promoted the solubility of CB[10] in DMSO. While the resonance peaks (H_a and H_b) of the 4,4′-bipyridine-1,1′-diium unit were shifted upfield of 0.93 and 0.74 ppm, the resonance peaks (H_c and H_d) of TPE units near the 4,4′-bipyridine-1,1′-diium unit slightly shifted downfield of 0.09 ppm and upfield of 0.08 ppm, respectively. Compared with free CB[10], all the resonance peaks of bound CB[10] showed a slight upfield shift (0.04–0.08 ppm). Based on these NMR shifts, the 4,4′-bipyridine-1,1′-diium unit of **1** is exactly anchored inside the cavity of CB[10]. Figure S7 shows side views of the electrostatic potential energy mapped onto the van der Waals surface of **1** and CB[10]·**1** complex. Obviously, the formation of the CB[10]·**1** complex results in substantial reduction in the electrostatic potential at the N atoms on the 4,4′-bipyridine-1,1′-ium unit as a consequence of the C═O···N$^+$ ion–dipole interactions.[17a]

In addition, the COSY and NOESY spectra also revealed the supramolecular assembled structure of rotaxane CB[10]·**1** in the solution (Figures S8–S9). An ESI-MS spectrum further showed that a double-charged peak of rotaxane CB[10]·**1** (m/z = 1239.9350) was consistent with the simulated peak of $[CB[10]\cdot\mathbf{1}]^{2+}$ (m/z = 1239.9292, Figure S10). All evidence of NMR and ESI-MS confirm that CB[10] can slip into the middle of dumbbell-like guest **1** under heating in DMSO and bind with the 4,4′-bipyridine-1,1′-diium unit by the C═O···N$^+$ ion–dipole interactions to form a stable CB[10]-based [2]rotaxane. However, guest **2** cannot thread through CB[10] to form the rotaxane under the same conditions, due to the inappropriate size of the dimethyl TPE units (Figure S11).

Aggregation-Induced Emission Enhancement of CB[10]·1. TPE derivatives with a unique AIE property have been widely used as a building block for fabricating fluorescent materials.[12] Furthermore, the host–guest recognitions have been demonstrated to be an efficient tool to realize RIR of the TPE unit in the limited cavity of the host.[35−46] Therefore, we decided to investigate the fluorescent emission properties of rotaxane CB[10]·**1** by fluorescence experiments. Interestingly, **1** exhibits highly selective fluorescence enhancement with CB[10] in DMSO solution due to the formation of [2]rotaxane CB[10]·**1**. As shown in Figure 3a, **1** is nonfluorescent in DMSO. Meanwhile CB[n] (n = 6–8) have almost no effect on the fluorescence emission because these hosts cannot encapsulate **1**. When CB[10] slipped to the middle of **1** with binding the 4,4′-bipyridine-1,1′-diium unit to form [2]rotaxane CB[10]·**1**; however, the fluorescent emission was obviously turned on with yellow color (λ_{em} = 558 nm) (Figure 3a). This fluorescence turn-on phenomenon could be attributed to the formation of CB[10]·**1**, which resulted in the restriction of intramolecular rotation of TPE (First step in Scheme 1). Furthermore, quantum yields and the fluorescence lifetime for CB[10]·**1** were measured in DMSO, as shown in Table S1. The quantum yield of CB[10]·**1** increased up to Φ = 0.50 in DMSO, while CB[10]·**1** displayed only one decay kinetics with contribution from a lifetime of 3.33 ns in DMSO (Figure S12). UV–vis spectra also showed that only CB[10] can bind **1** to form rotaxane, resulting in a blue shift ($\Delta\lambda$ = 32 nm) of the absorption maximun (Figure 3b).

Due to the AIE property of the TPE unit, we envisioned that the concentration of CB[10]·**1** and the addition of other solvents with low or high polarity should control the aggregation of CB[10]·**1** in the solution phase to exhibit stronger emission properties. The fluorescence intensity of CB[10]·**1** in DMSO increased linearly as the concentration of CB[10]·**1** was gradually increased from 2.0 to 28.8 μM, and then showed little change up to 100 μM, which implies that the critical aggregate concentration of CB[10]·**1** in DMSO is around 28.8 μM (Figure S13). Furthermore, fluorescent emission of **1** and CB[10]·**1** were recorded by adding 10 different solvents including polar and nonpolar solvents (Figure

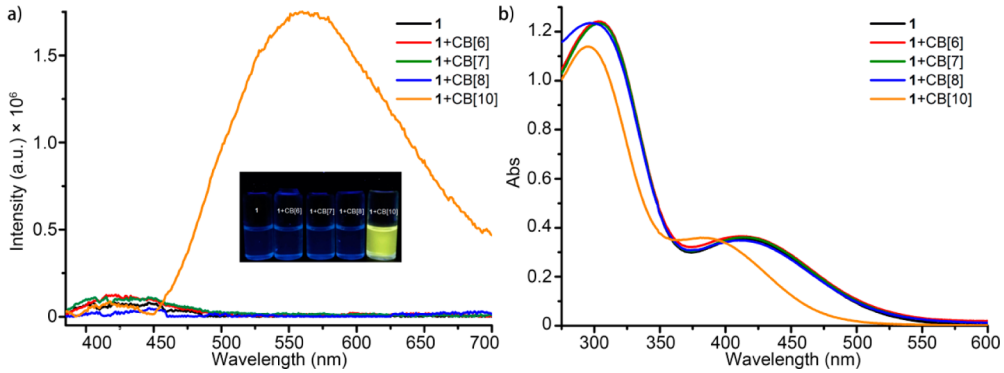

Figure 3. (a) Fluorescence spectra of **1** (10 μM) and b) UV–vis spectra of **1** (50 μM) without and with 1 equiv of CB[n] (n = 6–8, 10) in DMSO, under heating at 95 °C for 17 days; insert photo: pictures of **1**, **1** + CB[6], **1** + CB[7], **1** + CB[8], and **1** + CB[10] in DMSO under a 365 nm lamp. λ_{ex} = 365 nm; Ex/Em slits = 5/5 nm.

DOI: 10.1021/acs.joc.7b00400
J. Org. Chem. 2017, 82, 5590–5596

Scheme 1. Cartoon Illustrations of a Stepwise Aggregation-Induced Emission Enhancement of CB[10]·1

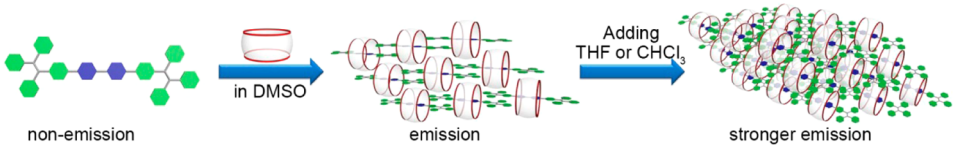

4). **1** showed the best fluorescence enhancement in 1,4-dioxane while CB[10]·**1** has the strongest fluorescent emission in

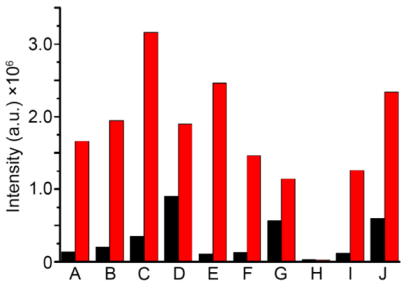

Figure 4. Fluorescence intensity at 600 nm of **1** (10 μM, black column) and CB[10]·**1** (10 μM, red column) in different solvents including 1% DMSO (A = acetone; B = CH_2Cl_2; C = $CHCl_3$; D = 1,4-dioxane; E = DMF; F = DMSO; G = EA; H = H_2O; I = MeOH; J = THF). λ_{ex} = 365 nm; Ex/Em slits = 5/5 nm.

$CHCl_3$ (Figures S14–S15). The quantum yield and lifetime of CB[10]·**1** in $CHCl_3$ are Φ = 0.78 and 2.50 ns (Figure S12). It is worthy to note that the fluorescent intensity of CB[10]·**1** is always stronger than that of **1** in different solvents, because these relaxation processes of TPE units are severely hindered by the hydrophobic cavity of CB[10] which enhances the AIE effect. It also indicated that the formation of CB[10]·**1** decreases the solubility in all solvents. Specifically, the fluorescent intensity of CB[10]·**1** in THF or $CHCl_3$ is obviously stronger than that in DMSO, which shows a stepwise aggregation-induced emission enhancement (second step in Scheme 1). In order to investigate the AIE property of CB[10]·**1**, further tests of the fluorescence were carried out in the mixed solvent of DMSO/H_2O. Figure S16 showed that when increasing the DMSO contents from 10% to 100%, fluorescent intensity with the emission maximum at 558 nm was increased gradually, which suggested that CB[10]·**1** had a strong AIE property. Compared with organic TPE deriveratives, both **1** and CB[10]·**1** showed weak fluorescence in water, probably because the H_2O molecules tend to favor bipyridine-1,1′-diium cations, resulting in disassembly of CH···π stacking between **1** molecules (Figure S17).

Aggregation Morphology of 1 and CB[10]·1. In order to further understand the aggregation behaviors of **1** and CB[10]·**1**, the dynamic light scattering (DLS) and the scanning electron microscopy (SEM) experiments were utilized. The aggregation transformation between **1** and CB[10]·**1** was evidenced by DLS experiments which revealed that the diameter (D) of aggregates of CB[10]·**1** in DMSO was ~396.1 nm at 0.10 mM and ~295.3 nm at 0.01 mM, respectively (Figures 5 and S18). These values are ~53 and ~39 times larger than that of **1** alone (~7.5 nm) which is consistent with the size of **1**. The DLS study confirmed again the aggregation of CB[10]·**1** in THF or $CHCl_3$ by demonstrating a huge increase of the hydrodynamic diameter of the species (~955.4 nm in THF; ~1106.0 nm in $CHCl_3$) in

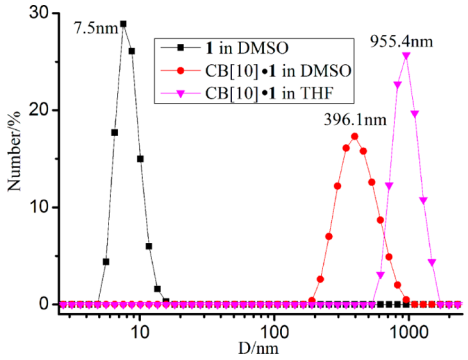

Figure 5. DLS profiles of **1** (0.10 mM) in DMSO and CB[10]·**1** (0.10 mM) in DMSO or THF including 10% DMSO.

the solution of CB[10]·**1** at the same concentration (Figures 5 and S19a). Therefore, the florescence enhancement of CB[10]·**1** after addition of THF or $CHCl_3$ could be attributed to more aggregation of CB[10]·**1**, which resulted in further inhibition of the rotation of TPE units in the stacked structures (Scheme 1).

The morphology of the aggregates formed from the solution of **1** or CB[10]·**1** were observed by SEM (Figure 6). The SEM images in Figure 6a–b show monodispersed spherical structures with a diameter ranging from 160 to 598 nm, probably due to the self-assembly between **1** molecules. As shown in Figure 6c–d, the well dispersed plate-like structure of CB[10]·**1** instead of the spherical structure of **1** was observed. It indicated that the formation of [2]rotaxane CB[10]·**1** could

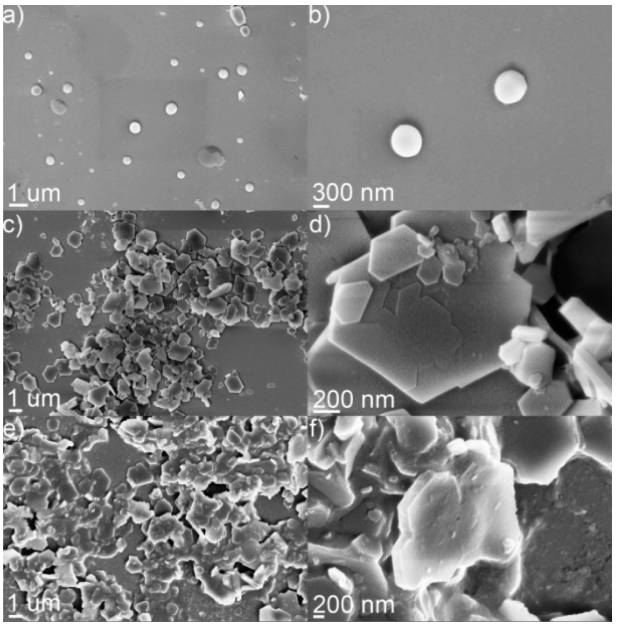

Figure 6. SEM images of the samples from (a and b) **1** (0.10 mM) in DMSO; (c and d) CB[10]·**1** (0.10 mM) in DMSO; and (e and f) CB[10]·**1** (0.10 mM) in THF including 10% DMSO.

DOI: 10.1021/acs.joc.7b00400
J. Org. Chem. 2017, 82, 5590–5596

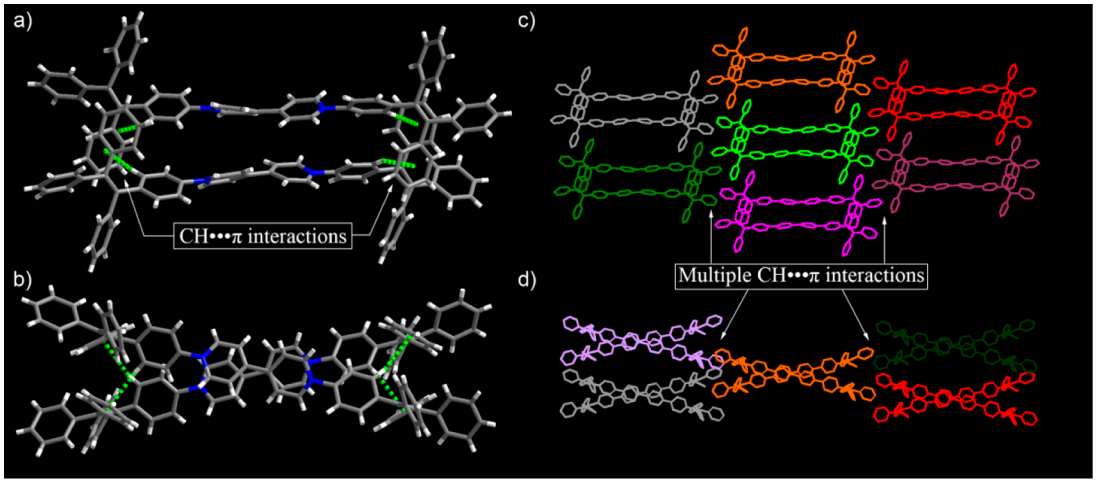

Figure 7. Crystal structure of **1**: (a) side view and (b) top view of face-to-face stacking dimer **1**•**1**; (c) side view and (d) top view of stacking networks between **1**•**1** dimers Color code: N, blue; O, red; C, gray; H, white. CH···π interactions: green dot line. Chloride ions to balance the charge are omitted.

convert the spherical self-assembled structure of **1** into the plate-like self-assembled structure of CB[10]·**1**, with accompanying fluorescence enhancement. Interestingly, the dispersed plate-like structures were combined with each other to form larger stacked structures in THF (Figure 6e–f) or $CHCl_3$ (Figure S19b–c).

X-ray Crystal Structure of 1. To understand the relationship between fluorescence enhancement and aggregation, we turned to X-ray analysis. We were fortunate to obtain X-ray quality crystals of **1** as red plates from 4:1 (v/v) MeOH/DMF solution by slow vapor diffusion of iPr$_2$O at room temperature. First, Figure 7a–b illustrate the dimerization of **1** to yield a bimolecular structure **1**•**1** by CH···π interactions between tetraphenylethylene units (Table S2). The dihedral angle of two pyridine rings in 4,4′-bipyridine-1,1′-diium units of **1** are about 33.1°. Although the 4,4′-bipyridine-1,1′-diium units in two different molecules are not parallel, the face-to-face stacking of **1**•**1** is stabilized by four CH···π interactions among tetraphenylethylene units. Subsequently, as shown in Figure 7c–d, the dimer **1**•**1** engages other **1**•**1** dimers through CH···π interactions among tetraphenylethylene units along with b axis (Figure S20a) and c axis (Figure S20b), respectively, to form a 3D network-like arrangement. Therefore, the X-ray structure of **1** further confirms that the aggregation of CB[10]•**1** could be stabilized by multiple CH···π interactions between tetraphenylethylene stoppers of CB[10]•**1** and exhibit a stepwise AIEE effect in THF or $CHCl_3$.

CONCLUSIONS

In summary, we have designed and synthesized a dumbbell-like guest **1** which is nonfluorescent but becomes a highly fluorescent [2]rotaxane CB[10]·**1** upon host–guest interaction with CB[10] via the slipping method under heating at 95 °C in DMSO. The photophysical properties and aggregation structures of **1** and CB[10]·**1** were unambiguously elucidated by fluorescence, UV–vis, DLS, SEM, and X-ray experiments. We are able to demonstrate that the formation of CB[10]·**1** is accompanied by strong fluorescent intensity, a long lifetime, and high quantum yield. Compared with **1**, CB[10]·**1** also exhibits a stepwise aggregation-induced emission enhancement property in THF or $CHCl_3$. Therefore, the supramolecular assembly strategy to prepare luminescent systems, which are easily endowed with multiple emission properties, may find useful application not only in luminescent materials but also in stimuli-responsive systems and molecular machines.

EXPERIMENTAL SECTION

General Experimental Methods. Starting materials were purchased from commercial suppliers and used without further purification. CB[n] (n = 6,[47] 7,[48] 8,[48] 10[28b]) was prepared according to the published procedure. Melting points were determined using the XT-4 apparatus. IR spectra were recorded on a Bruker IFS 120HR spectrometer and were reported in cm^{-1}. ^{1}H NMR and ^{13}C NMR spectra were obtained on a Bruker ascend spectrometer at 400 MHz. Electron Spray Ionization (ESI) mass spectra were acquired by using a Bruker micrOTOF-Q II electrospray instrument. Fluorescence spectra were recorded on a Horiba Fluorolog-3 spectrometer equipped with a xenon discharge lamp using 1 cm quartz cells. DLS data were recorded on a Malvern Zetasizer nano ZS90 spectrometer using a monochromatic coherent He–Ne laser (633 nm) as the light source and a detector that detected the scattered light at an angle of 90°. SEM images were obtained on Carl Zeiss SIGMA.

Fluorescence Measurement. Fluorescence spectra were obtained with a solution of **1** (3 mL, 10 μM) or CB[10]·**1** (3 mL, 10 μM) in a quartz cell. The solution of CB[10]·**1** (1.0 mM) in DMSO was prepared after being heated at 95 °C for 17 days. The different solvents were added to the DMSO solution of CB[10]·**1** (1.0 mM) to change the ratio of DMSO to 1%.

Scanning Electron Microscope Measurement. One drop of the solution of **1** (0.10 mM) or CB[10]·**1** (0.10 mM) was placed on the silicon wafer and dried for 1 day under heating at 50 °C. The samples were then coated with Au in the ion coater for 90 s. The solution of CB[10]·**1** (1.0 mM) in DMSO was prepared after being heated at 95 °C for 17 days. The different solvents were added to the DMSO solution of CB[10]·**1** (1.0 mM) to change the ratio of DMSO to 10%.

Dynamic Light Scattering Measurement. DLS data were obtained with a solution of **1** (1 mL, 0.10 mM) or CB[10]·**1** (1 mL, 0.10 mM or 0.01 mM) in a quartz cell. The solution of CB[10]·**1** (1.0 mM) in DMSO was prepared after being heated at 95 °C for 17 days. The different solvents were added to the DMSO solution of CB[10]·**1** (1.0 mM) to change the ratio of DMSO to 10%.

Synthetic Procedures. *Compound 1.* A mixture of 4-(1,2,2-triphenylvinyl)aniline (384 mg, 1.10 mmol) and 1,1′-bis(2,4-dinitrophenyl)-[4,4′-bipyridine]-1,1′-diium chloride (281.8 mg, 0.50 mmol) in ethanol (25 mL) was heated at reflux for 3 days. After cooling down to room temperature, the product was precipitated with diethyl ether and washed with diethyl ether and acetone to yield **1** as a red solid (427 mg, 0.48 mmol, 96%). Mp 248–249 °C. IR (KBr,

DOI: 10.1021/acs.joc.7b00400
J. Org. Chem. 2017, 82, 5590–5596

cm^{-1}): 3401s, 3108m, 3052m, 3020m, 1630s, 1485m, 1436m, 761w, 698s. ^{1}H NMR (400 MHz, DMSO-d_6): 9.62 (d, J = 6.8 Hz, 4H), 9.01 (d, J = 6.8 Hz, 4H), 7.77 (d, J = 8.6 Hz, 4H), 7.38 (d, J = 8.6 Hz, 4H), 7.25−7.00 (m, 30H). ^{13}C NMR (100 MHz, DMSO-d_6): 148.6, 146.7, 145.5, 142.7, 142.5, 142.5, 140.1, 138.7, 132.3, 130.7, 130.5, 128.2, 128.1, 127.9, 127.2, 127.0, 126.6, 124.2 (only 18 of the 21 resonances expected were observed). HRMS (ESI-TOF) m/z: [**1** − 2Cl$^-$]$^{2+}$ calcd for $C_{62}H_{46}N_2$ 409.1825; found 409.1819.

Compound **2**. A mixture of compound 4-(1-phenyl-2,2-di-*p*-tolylvinyl)aniline (100 mg, 0.27 mmol) and 1,1′-bis(2,4-dinitrophenyl)-[4,4′-bipyridine]-1,1′-diium chloride (67.9 mg, 0.12 mmol) in ethanol (10 mL) was heated at reflux for 3 days. After cooling down to room temperature, the solvent was reduced, and the product was dissolved in acetone and then precipitated with diethyl ether and washed with diethyl ether to yield **2** as a red solid (90 mg, 0.10 mmol, 83.3%). Mp 200−201 °C. IR (KBr, cm^{-1}): 3409s, 3021m, 2917m, 1604s, 1499m, 1443m, 1306m, 822w, 668w. ^{1}H NMR (400 MHz, DMSO-d_6): 9.63 (d, J = 6.8, 4H), 9.01 (d, J = 6.8, 4H), 7.77 (d, J = 8.6, 4H), 7.35 (d, J = 8.6, 4H), 7.25−6.85 (m, 26H), 2.23 (s, 6H), 2.21 (s, 6H). ^{13}C NMR (100 MHz, DMSO-d_6): 147.0, 145.5, 142.9, 142.4, 139.9, 139.7, 137.8, 136.3, 136.1, 132.3, 130.7, 130.6, 128.8, 128.5, 128.1, 126.8, 126.6, 124.2, 20.8, 20.7. HRMS (ESI-TOF) m/z: [**2** − 2Cl$^-$]$^{2+}$ Calcd for $C_{66}H_{54}N_2$ 437.2138; Found 437.2144.

■ ASSOCIATED CONTENT

Supporting Information

The Supporting Information is available free of charge on the ACS Publications website at DOI: 10.1021/acs.joc.7b00400.

NMR data, ESI-MS data, fluorescent spectra, UV−vis spectra, SEM, DLS, and X-ray data (PDF)

Crystallographic data for CCDC-1511208 (CIF)

■ AUTHOR INFORMATION

Corresponding Authors

*E-mail: liusimin@wust.edu.cn.

*E-mail: chcaoliping@nwu.edu.cn.

ORCID

Simin Liu: 0000-0002-8696-4833

Liping Cao: 0000-0002-1747-6107

Author Contributions

§Y.Y. and Y.L. contributed equally.

Notes

The authors declare no competing financial interest.

■ ACKNOWLEDGMENTS

We thank the National Natural Science Foundation of China (21472149 to L.C., 21472143 to S.L.), the Shaanxi Provincial Natural Science Foundation (2016JM2025, 2016JQ2015 to Y.Z.), and Research Project of Shaanxi Provincial Education Department (15Js112) for financial support.

■ REFERENCES

(1) (a) Goldenberg, L. M.; Lisinetskii, V.; Gritsai, Y.; Stumpe, J.; Schrader, S. *Adv. Mater.* **2012**, *24*, 3339−3343. (b) Chen, C. Y.; Lee, W. K.; Chen, Y. J.; Lu, C. Y.; Lin, H. Y.; Wu, C. C. *Adv. Mater.* **2015**, *27*, 4883−4888.

(2) Jiang, B.-P.; Guo, D.-S.; Liu, Y.-C.; Wang, K.-P.; Liu, Y. *ACS Nano* **2014**, *8*, 1609−1618.

(3) Kobayashi, H.; Choyke, P. L. *Acc. Chem. Res.* **2011**, *44*, 83−90.

(4) Li, D.; Song, S. P.; Fan, C. H. *Acc. Chem. Res.* **2010**, *43*, 631−641.

(5) Shi, H. B.; Liu, J. Z.; Geng, J. L.; Tang, B. Z.; Liu, B. *J. Am. Chem. Soc.* **2012**, *134*, 9569−9572.

(6) Song, Q.; Li, F.; Wang, Z. Q.; Zhang, X. *Chem. Sci.* **2015**, *6*, 3342−3346.

(7) Qian, H.; Cousins, M. E.; Horak, E. H.; Wakefield, A.; Liptak, M. D.; Aprahamian, I. *Nat. Chem.* **2016**, *9*, 83−87.

(8) Maggini, L.; Bonifazi, D. *Chem. Soc. Rev.* **2012**, *41*, 211−241.

(9) Licchelli, M.; Biroli, A. O.; Poggi, A. *Org. Lett.* **2006**, *8*, 915−918.

(10) Ajami, D.; Schramm, M. P.; Volonterio, A.; Rebek, J., Jr. *Angew. Chem., Int. Ed.* **2007**, *46*, 242−244.

(11) Birks, J. B. *Photophysics of Aromatic Molecules*; Wiley: London, 1970.

(12) (a) Hong, Y.; Lam, J. W. Y.; Tang, B. Z. *Chem. Soc. Rev.* **2011**, *40*, 5361−5388. (b) Hong, Y.; Lam, J. W. Y.; Tang, B. Z. *Chem. Commun.* **2009**, 4332−4353.

(13) (a) Jelley, E. E. *Nature* **1936**, *138*, 1009−1010. (b) West, W.; Geddes, A. L. *J. Phys. Chem.* **1964**, *68*, 837−847. (c) Halterman, R. L.; Moore, J. L.; Mannel, L. M. *J. Org. Chem.* **2008**, *73*, 3266−3269. (d) Xie, Z.; Stepanenko, V.; Radacki, K.; Würthner, F. *Chem. - Eur. J.* **2012**, *18*, 7060−7070. (e) Wang, Y. J.; Li, Z.; Tong, J.; Shen, X. Y.; Qin, A.; Sun, J. Z.; Tang, B. Z. *J. Mater. Chem. C* **2015**, *3*, 3559−3568.

(14) Song, Q.; Jiao, Y.; Wang, Z. Q.; Zhang, X. *Small* **2016**, *12*, 24−31.

(15) Peng, H. Q.; Niu, L. Y.; Chen, Y. Z.; Wu, L. Z.; Tung, C. H.; Yang, Q. Z. *Chem. Rev.* **2015**, *115*, 7502−7542.

(16) (a) Lagona, J.; Mukhopadhyay, P.; Chakrabarti, S.; Isaacs, L. *Angew. Chem., Int. Ed.* **2005**, *44*, 4844−4870. (b) Assaf, K. I.; Nau, W. M. *Chem. Soc. Rev.* **2015**, *44*, 394−418. (c) Cong, H.; Ni, X. L.; Xiao, X.; Huang, Y.; Zhu, Q.-J.; Xue, S.-F.; Tao, Z.; Lindoy, L. F.; Wei, G. *Org. Biomol. Chem.* **2016**, *14*, 4335−4364. (d) Masson, E.; Ling, X.; Joseph, R.; Kyeremeh-Mensah, L.; Lu, X. *RSC Adv.* **2012**, *2*, 1213−1247.

(17) (a) Cao, L.; Sekutor, M.; Zavalij, P. Y.; Mlinaric-Majerski, K.; Glaser, R.; Isaacs, L. *Angew. Chem., Int. Ed.* **2014**, *53*, 988−993. (b) Barrow, S. J.; Kasera, S.; Rowland, M. J.; del Barrio, J.; Scherman, O. A. *Chem. Rev.* **2015**, *115*, 12320−12406.

(18) (a) Vinciguerra, B.; Cao, L.; Cannon, J. R.; Zavalij, P. Y.; Fenselau, C.; Isaacs, L. *J. Am. Chem. Soc.* **2012**, *134*, 13133−13140. (b) Cao, L.; Isaacs, L. *Org. Lett.* **2012**, *14*, 3072−3075. (c) Roh, S.-G.; Park, K.-M.; Park, G.-J.; Sakamoto, S.; Yamaguchi, K.; Kim, K. *Angew. Chem., Int. Ed.* **1999**, *38*, 637−641. (d) Zhao, N.; Lloyd, G. O.; Scherman, O. A. *Chem. Commun.* **2012**, *48*, 3070−3072.

(19) (a) Lee, T.-C.; Kalenius, E.; Lazar, A. I.; Assaf, K. I.; Kuhnert, N.; Grun, C. H.; Janis, J.; Scherman, O. A.; Nau, W. M. *Nat. Chem.* **2013**, *5*, 376−382. (b) Lu, X.; Masson, E. *Org. Lett.* **2010**, *12*, 2310−2313.

(20) (a) Ghale, G.; Nau, W. M. *Acc. Chem. Res.* **2014**, *47*, 2150−2159. (b) Minami, T.; Esipenko, N. A.; Zhang, B.; Kozelkova, M. E.; Isaacs, L.; Nishiyabu, R.; Kubo, Y.; Anzenbacher, P. *J. Am. Chem. Soc.* **2012**, *134*, 20021−20024.

(21) (a) Cao, L.; Hettiarachchi, G.; Briken, V.; Isaacs, L. *Angew. Chem., Int. Ed.* **2013**, *52*, 12033−12037. (b) Uzunova, V. D.; Cullinane, C.; Brix, K.; Nau, W. M.; Day, A. I. *Org. Biomol. Chem.* **2010**, *8*, 2037−2042. (c) Ma, D.; Hettiarachchi, G.; Nguyen, D.; Zhang, B.; Wittenberg, J. B.; Zavalij, P. Y.; Briken, V.; Isaacs, L. *Nat. Chem.* **2012**, *4*, 503−510. (d) Appel, E. A.; Rowland, M. J.; Loh, X. J.; Heywood, R. M.; Watts, C.; Scherman, O. A. *Chem. Commun.* **2012**, *48*, 9843−9845.

(22) Appel, E. A.; Biedermann, F.; Rauwald, U.; Jones, S. T.; Zayed, J. M.; Scherman, O. A. *J. Am. Chem. Soc.* **2010**, *132*, 14251−14260.

(23) Kim, K. *Chem. Soc. Rev.* **2002**, *31*, 96−107.

(24) (a) Chen, K.; Kang, Y. S.; Zhao, Y.; Yang, J. M.; Lu, Y.; Sun, W. Y. *J. Am. Chem. Soc.* **2014**, *136*, 16744−16747. (b) Zhang, K.-D.; Tian, J.; Hanifi, D.; Zhang, Y.; Sue, A. C.-H.; Zhou, T.-Y.; Zhang, L.; Zhao, X.; Liu, Y.; Li, Z.-T. *J. Am. Chem. Soc.* **2013**, *135*, 17913−17918. (c) Tian, J.; Zhou, T.-Y.; Zhang, S.-C.; Aloni, S.; Altoe, M. V.; Xie, S.-H.; Wang, H.; Zhang, D.-W.; Zhao, X.; Liu, Y.; Li, Z.-T. *Nat. Commun.* **2014**, *5*, 5574−5584.

(25) (a) Bhasikuttan, A. C.; Mohanty, J.; Nau, W. M.; Pal, H. *Angew. Chem., Int. Ed.* **2007**, *46*, 4120−4122. (b) Biedermann, F.; Elmalem, E.; Ghosh, I.; Nau, W. M.; Scherman, O. A. *Angew. Chem., Int. Ed.* **2012**, *51*, 7739−7743. (c) Freitag, M.; Gundlach, L.; Piotrowiak, P.; Galoppini, E. *J. Am. Chem. Soc.* **2012**, *134*, 3358−3366. (d) Kim, H.-J.;

DOI: 10.1021/acs.joc.7b00400
J. Org. Chem. 2017, 82, 5590−5596

Whang, D. R.; Gierschner, J.; Park, S. Y. *Angew. Chem., Int. Ed.* **2016**, *55*, 15915−15919.
(26) Ni, X. L.; Chen, S. Y.; Yang, Y. P.; Tao, Z. *J. Am. Chem. Soc.* **2016**, *138*, 6177−6183.
(27) Gadde, S.; Batchelor, E. K.; Weiss, J. P.; Ling, Y.; Kaifer, A. E. *J. Am. Chem. Soc.* **2008**, *130*, 17114−17119.
(28) (a) Day, A. I.; Blanch, R. J.; Arnold, A. P.; Lorenzo, S.; Lewis, G. R.; Dance, I. *Angew. Chem., Int. Ed.* **2002**, *41*, 275−277. (b) Liu, S.; Zavalij, P. Y.; Isaacs, L. *J. Am. Chem. Soc.* **2005**, *127*, 16798−16799. (c) Liu, S.; Zavalij, P. Y.; Lam, Y.-F.; Isaacs, L. *J. Am. Chem. Soc.* **2007**, *129*, 11232−11241. (d) Liu, S.; Shukla, A. D.; Gadde, S.; Wagner, B. D.; Kaifer, A. E.; Isaacs, L. *Angew. Chem., Int. Ed.* **2008**, *47*, 2657−2660. (e) Pisani, M. J.; Zhao, Y.; Wallace, L.; Woodward, C. E.; Keene, F. R.; Day, A. I.; Collins, J. G. *Dalton Trans.* **2010**, *39*, 2078−2086. (f) Li, F.; Feterl, M.; Warner, J. M.; Day, A. I.; Keene, F. R.; Collins, J. G. *Dalton Trans.* **2013**, *42*, 8868−8877. (g) Alrawashdeh, L. R.; Day, A. I.; Wallace, L. *Dalton Trans.* **2013**, *42*, 16478−16481. (h) Gong, W.; Yang, X.; Zavalij, P. Y.; Isaacs, L.; Zhao, Z.; Liu, S. *Chem. - Eur. J.* **2016**, *22*, 17612−17618.
(29) (a) Harrison, I. T.; Harrison, S. *J. Am. Chem. Soc.* **1967**, *89*, 5723−5724. (b) Bravo, J. A.; Raymo, F. M.; Stoddart, J. F.; White, A. J. P.; Williams, D. J. *Eur. J. Org. Chem.* **1998**, *1998*, 2565−2571.
(30) (a) Whang, D.; Jeon, Y.-M.; Heo, J.; Kim, K. *J. Am. Chem. Soc.* **1996**, *118*, 11333−11334. (b) Whang, D.; Heo, J.; Kim, C.-A.; Kim, K. *Chem. Commun.* **1997**, 2361−2362.
(31) (a) Whang, D.; Kim, K. *J. Am. Chem. Soc.* **1997**, *119*, 451−452. (b) Lee, E.; Kim, J.; Heo, J.; Whang, D.; Kim, K. *Angew. Chem., Int. Ed.* **2001**, *40*, 399−402.
(32) (a) Lee, E.; Heo, J.; Kim, K. *Angew. Chem., Int. Ed.* **2000**, *39*, 2699−2701. (b) Liang, J.; Wang, X.-L.; Jiao, Y.-Q.; Qin, C.; Shao, K.-Z.; Su, Z.-M.; Wu, Q.-Y. *Chem. Commun.* **2013**, *49*, 8555−8557. (c) Li, J.; Zhao, Y.; Dong, Y.; Yu, Y.; Cao, L.; Wu, B. *CrystEngComm* **2016**, *18*, 7929−7933.
(33) (a) Whang, D.; Park, K.-M.; Heo, J.; Ashton, P.; Kim, K. *J. Am. Chem. Soc.* **1998**, *120*, 4899−4900. (b) Roh, S.-G.; Park, K.-M.; Park, G.-J.; Sakamoto, S.; Yamaguchi, K.; Kim, K. *Angew. Chem., Int. Ed.* **1999**, *38*, 637−641. (c) Park, K.-M.; Kim, S.-Y.; Heo, J.; Whang, D.; Sakamoto, S.; Yamaguchi, K.; Kim, K. *J. Am. Chem. Soc.* **2002**, *124*, 2140−2147. (d) Ko, Y. H.; Kim, K.; Kang, J.-K.; Chun, H.; Lee, J. W.; Sakamoto, S.; Yamaguchi, K.; Fettinger, J. C.; Kim, K. *J. Am. Chem. Soc.* **2004**, *126*, 1932−1933. (e) Li, J.; Yu, Y.; Luo, L.; Li, Y.; Wang, P.; Cao, L.; Wu, B. *Tetrahedron Lett.* **2016**, *57*, 2306−2310.
(34) Moon, K.; Kaifer, A. E. *Org. Lett.* **2004**, *6*, 185−188.
(35) Song, S.; Zheng, H.-F.; Li, D.-M.; Wang, J.-H.; Feng, H.-T.; Zhu, Z.-H.; Chen, Y.-C.; Zheng, Y.-S. *Org. Lett.* **2014**, *16*, 2170−2173.
(36) Xu, S.-Q.; Zhang, X.; Nie, C.-B.; Pang, Z.-F.; Xu, X.-N.; Zhao, X. *Chem. Commun.* **2015**, *51*, 16417−16420.
(37) Jiang, R.; Wang, S.; Li, J. *RSC Adv.* **2016**, *6*, 4478−4482.
(38) Liang, G.; Lam, J. W. Y.; Qin, W.; Li, J.; Xie, N.; Tang, B. Z. *Chem. Commun.* **2014**, *50*, 1725−1727.
(39) Jiang, B.-P.; Guo, D.-S.; Liu, Y.-C.; Wang, K.-P.; Liu, Y. *ACS Nano* **2014**, *8*, 1609−1618.
(40) Yao, X.; Ma, X.; Tian, H. *J. Mater. Chem. C* **2014**, *2*, 5155−5160.
(41) Wang, P.; Yan, X.; Huang, F. *Chem. Commun.* **2014**, *50*, 5017−5019.
(42) Yu, G.; Tang, G.; Huang, F. *J. Mater. Chem. C* **2014**, *2*, 6609−6617.
(43) Wu, J.; Sun, S.; Feng, X.; Shi, J.; Hu, X.-Y.; Wang, L. *Chem. Commun.* **2014**, *50*, 9122−9125.
(44) Song, N.; Chen, D.-X.; Qiu, Y.-C.; Yang, X.-Y.; Xu, B.; Tian, W.; Yang, Y.-W. *Chem. Commun.* **2014**, *50*, 8231−8234.
(45) Bai, W.; Wang, Z.; Tong, J.; Mei, J.; Qin, A.; Sun, J. Z.; Tang, B. Z. *Chem. Commun.* **2015**, *51*, 1089−1091.
(46) Liu, Y.-C.; Wang, Y.-Y.; Tian, H.-W.; Liu, Y.; Guo, D.-S. *Org. Chem. Front.* **2016**, *3*, 53−61.
(47) Freeman, W. A.; Mock, W. L.; Shih, N.-Y. *J. Am. Chem. Soc.* **1981**, *103*, 7367−7368.
(48) Kim, J.; Jung, I.-S.; Kim, S.-Y.; Lee, E.; Kang, J.-K.; Sakamoto, S.; Yamaguchi, K.; Kim, K. *J. Am. Chem. Soc.* **2000**, *122*, 540−541.

DOI: 10.1021/acs.joc.7b00400
J. Org. Chem. 2017, 82, 5590−5596